

1998


# Atomic Hydrogen Cleaning of InP(100) for Preparation of a Negative Electron Affinity Photocathode

K. A. Elamrawi  
*Old Dominion University*

M. A. Hafez  
*Old Dominion University*

H. E. Elsayed-Ali  
*Old Dominion University*, [helsayed@odu.edu](mailto:helsayed@odu.edu)

Follow this and additional works at: [https://digitalcommons.odu.edu/ece\\_fac\\_pubs](https://digitalcommons.odu.edu/ece_fac_pubs)

 Part of the [Electronic Devices and Semiconductor Manufacturing Commons](#), and the [Engineering Physics Commons](#)

## Repository Citation

Elamrawi, K. A.; Hafez, M. A.; and Elsayed-Ali, H. E., "Atomic Hydrogen Cleaning of InP(100) for Preparation of a Negative Electron Affinity Photocathode" (1998). *Electrical & Computer Engineering Faculty Publications*. 121.  
[https://digitalcommons.odu.edu/ece\\_fac\\_pubs/121](https://digitalcommons.odu.edu/ece_fac_pubs/121)

## Original Publication Citation

Elamrawi, K. A., Hafez, M. A., & Elsayed-Ali, H. E. (1998). Atomic hydrogen cleaning of InP(100) for preparation of a negative electron affinity photocathode. *Journal of Applied Physics*, 84(8), 4568-4572. doi:10.1063/1.368701

# Atomic hydrogen cleaning of InP(100) for preparation of a negative electron affinity photocathode

K. A. Elamrawi, M. A. Hafez, and H. E. Elsayed-Ali<sup>a)</sup>

*Department of Electrical and Computer Engineering, Old Dominion University, Norfolk, Virginia 23529*

(Received 25 June 1998; accepted for publication 20 July 1998)

Atomic hydrogen cleaning is used to clean InP(100) negative electron affinity photocathodes. Reflection high-energy electron diffraction patterns of reconstructed, phosphorus-stabilized, InP(100) surfaces are obtained after cleaning at  $\sim 400$  °C. These surfaces produce high quantum efficiency photocathodes ( $\sim 8.5\%$ ), in response to 632.8 nm light. Without atomic hydrogen cleaning, activation of InP to negative electron affinity requires heating to  $\sim 530$  °C. At this high temperature, phosphorus evaporates preferentially and a rough surface is obtained. These surfaces produce low quantum efficiency photocathodes ( $\sim 0.1\%$ ). The use of reflection high-energy electron diffraction to measure the thickness of the deposited cesium layer during activation by correlating diffraction intensity with photoemission is demonstrated. © 1998 American Institute of Physics. [S0021-8979(98)08620-4]

## I. INTRODUCTION

Indium phosphide has considerable applications in the manufacture of electronic and optoelectronic devices. It has a large thermal conductivity, and small electron diffusion that makes it preferable for transferred electron devices.<sup>1</sup> InP has been explored as a solar cell material since its energy gap is close to the optimum value for efficient conversion of solar radiation into electrical power by means of single-junction photovoltaic cells.<sup>1</sup> The energy band gap, lattice constant, and high optical absorption coefficient of InP make it a suitable photocathode material and a lattice-matched substrate for the growth of epitaxial layers of  $\text{Ga}_x\text{In}_{1-x}\text{P}_y\text{As}_{1-y}$ /InP heterostructures that have direct band gaps. These heterostructures have been employed to extend the sensitivity of photocathodes beyond the long wavelength limit of conventional devices,<sup>2</sup> and are presently considered for use as light sources and detectors for optical communication.<sup>3</sup>

InP is used for negative electron affinity (NEA) photocathodes.<sup>4-6</sup> These photocathodes have greatly improved the performance of many conventional light-sensing devices. They are widely used in low-light-level detection, such as scintillation counting, photomultipliers, and imaging devices.<sup>7</sup> NEA photocathodes were recently proposed for electron microscopy and high throughput electron-beam lithography, where isolated multilayer structures are integrated on the photocathode, while protecting the emission areas throughout the fabrication processes.<sup>8-10</sup> NEA photocathodes operate at room temperature, emit electrons with low energy spread, small angular spread, and low dark currents. NEA III-V semiconductor photocathodes produce spin polarized electrons, used in atomic, surface, and high-energy physics, when optically pumped by circularly polarized light.<sup>11</sup> Strained semiconductors can produce electron polarization as high as 80%.<sup>12</sup>

Heavily doped *p*-type InP is used as a photocathode material because its Fermi level is close to the valence band. This reduces the electron emission by purely thermal excitation. In positive electron affinity semiconductor surfaces, the vacuum level lies above the bulk conduction band minimum, and electrons excited from the valence band to the conduction band minimum cannot escape from the crystal surface. In NEA semiconductor surfaces, the vacuum level is lowered below the bulk conduction band minimum, and electrons excited to the conduction band minimum are emitted from the surface. The escape depth in this case is not limited by the mean-free path of the hot electrons, which is on the order of 10 nm, but by the diffusion length of the electrons thermalized to the conduction band minimum, which is on the order of several  $\mu\text{m}$ .<sup>13</sup> NEA photocathodes produce high quantum efficiency (QE), defined as the number of emitted electrons per incident photon, because of the lower vacuum level and the larger electron escape depth.

NEA surfaces are typically prepared by first cleaning the semiconductor surface chemically before loading it in ultra-high vacuum (UHV). Then the sample is heat cleaned in UHV to remove the surface contaminants. After the sample is cooled down to room temperature, activation to NEA is typically performed by the coadsorption of cesium and oxygen (or  $\text{NF}_3$ ) on the sample surface.<sup>14</sup> The photocathode lifetime depends on the light intensity, photoemitted current, accelerating voltage of the emitted electrons, and vacuum conditions. Longer lifetime is obtained under low level continuous cesiation.<sup>15</sup> The performance of the photocathode is significantly affected by the pressure in the UHV chamber, and a base pressure  $< 1 \times 10^{-9}$  Torr is required for long lifetime operation. After the QE drops to low values, the surface can be revived by further cesium deposition or by heat cleaning and reactivating with cesium and oxygen.

Preparation of a clean InP surface is of fundamental importance for NEA device fabrication. It is assumed that the effect of surface contamination is to form an interfacial potential barrier that does not allow the low energy electrons to

<sup>a)</sup> Author to whom correspondence should be addressed; electronic mail: elsayed-ali@ece.odu.edu

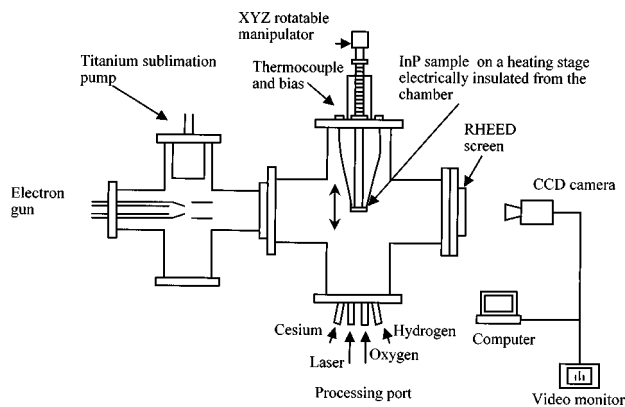


FIG. 1. Ultrahigh vacuum chamber for photocathode preparation. The processing port includes a port for oxygen, atomic hydrogen source, cesium evaporation, and a window for passing the laser to the sample.

escape into vacuum, thus increasing the surface trapping coefficient. This barrier decreases the photoemission sensitivity and produces low QE photocathodes.<sup>16</sup> The main contaminants observed on InP surfaces are carbon and oxygen.<sup>3</sup> Native oxides are desorbed by heating to  $\sim 500\text{--}530\text{ }^\circ\text{C}$ , a temperature much higher than InP congruent temperature ( $\sim 400\text{ }^\circ\text{C}$ ).<sup>17,18</sup> Moreover, it is difficult to completely remove carbon contaminants from the surface by thermal cleaning. When the InP surface temperature is below the congruent temperature, indium and phosphorus evaporate in equal proportions and the InP surface is phosphorus stabilized. These surfaces when activated to NEA, produce high QE photocathodes. If the InP surface is heated above the congruent temperature, phosphorus evaporates preferentially, leaving indium droplets on the surface. These surfaces produce very low QE photocathodes. In addition, heat cleaning above the congruent temperature results in a rough surface which affects the collimation of the emitted beam by increasing the angular spread of the emitted electrons and thus limits the application of NEA photocathodes in electron-beam lithography and microelectronics applications.<sup>11</sup> Strained semiconductors, used to obtain highly polarized photoelectrons, are affected by high temperature cleaning. Strain relief occurs due to the formation of dislocations and defects that lead to decreased value of electron polarization.<sup>13</sup>

Recently, atomic hydrogen irradiation has been studied as a surface cleaning method.<sup>3,17-20</sup> In addition to removal of surface contaminants, exposure to atomic hydrogen leads to the passivation of donors and acceptors in certain doped semiconductors,<sup>21</sup> acts as a surfactant during epitaxial growth,<sup>22</sup> and reduces dislocation densities at heteroepitaxial semiconductor surfaces.<sup>23</sup> Surface cleaning of III-V semiconductors has been previously reported using a variety of atomic hydrogen sources. These include rf discharge,<sup>20</sup> electron cyclotron resonance discharge,<sup>24</sup> and a hydrogen thermal cracking source.<sup>3</sup> Hydrogen plasma has energetic ions (up to  $\sim 100\text{ eV}$ ) which can cause physical and electronic damage to the surface extending several hundred  $\text{\AA}$  into the bulk. Normal incidence irradiation using a hydrogen plasma source produced more surface damage than grazing incidence irradiation.<sup>25</sup> In contrast, cracking sources produce atomic hydrogen with kinetic energies thermalized with the

ambient gas. For InP, atomic hydrogen cleaning can be accomplished at a surface temperature  $\sim 350\text{--}400\text{ }^\circ\text{C}$ . In addition to the cleaning effect, atomic hydrogen promotes a homogeneous oxide desorption resulting in a smooth phosphorus stabilized surface. Auger analysis of InP surfaces shows complete removal of carbon and oxygen after hydrogen cleaning.<sup>3</sup>

We have previously used atomic hydrogen for preparing GaAs photocathodes.<sup>26</sup> We obtained QE of  $\sim 12\%$  in response to  $632.8\text{ nm}$  light. Here, we report on the use of atomic hydrogen produced in a thermal cracking source for cleaning InP NEA photocathodes. We study the effect of atomic hydrogen cleaning on the performance of InP NEA photocathodes and determine the optimum cleaning temperature range. After atomic hydrogen cleaning, reflection high energy electron diffraction (RHEED) studies show that the InP(100) is a reconstructed, phosphorus stabilized surface, and produces a high QE of  $\sim 8.5\%$  in response to  $632.8\text{ nm}$  light. When heated to  $530\text{ }^\circ\text{C}$ , the RHEED patterns show an atomically rough surface as a result of preferential desorption of phosphorus leading to very low QE, when activated to NEA.

## II. EXPERIMENT

The work is carried out in a stainless steel UHV chamber (shown in Fig. 1) which is pumped by a  $220\text{ l/s}$  ion pump, and a titanium sublimation pump to the mid  $10^{-10}$  Torr range. The InP substrate is mounted on a molybdenum plate on top of a resistive heater that can be heated up to  $600\text{ }^\circ\text{C}$ . The sample is fixed with two molybdenum clamps. A thermocouple is attached to the sample holder close to the sample in order to measure its temperature. A wire is connected to the sample holder to allow applying a voltage bias to the sample for photocurrent measurement. The sample holder is connected to a xyz manipulator through a ceramic rod that provides electrical insulation of the sample from the chamber walls, used as the anode for the negatively biased sample. The manipulator also provides azimuthal rotation which is used to set the direction of the incident electron beam when acquiring the RHEED patterns. The UHV chamber is equipped with a RHEED gun and a phosphorus screen. The substrate faces a processing port which has a port to deposit cesium during NEA activation, a leak valve for oxygen admission, a glass window to allow the laser light to activate the InP photocathode, and a port for the hydrogen cracking source. RHEED patterns are acquired by a charge coupled device (CCD) detector connected to a computer and a video monitor. This image analysis system is similar to that used in Ref. 27. The hydrogen cracking source consists of a tungsten filament inserted in a boron nitride tube. The molecular hydrogen is introduced through a leak valve and passes in the boron nitride tube where it becomes partially dissociated and the atomic hydrogen is transported to the sample. The hydrogen pressure during the cleaning process is  $\sim 1 \times 10^{-6}$  Torr. The dissociation efficiency is estimated to be  $\sim 3\%$  based on the filament temperature.<sup>28</sup>

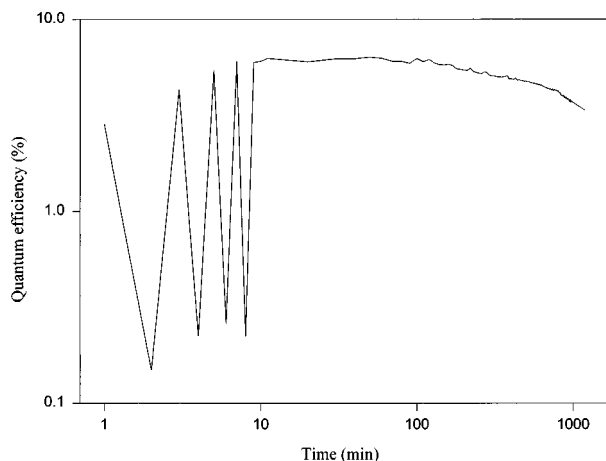


FIG. 2. Typical photoresponse of InP photocathode activated to negative electron affinity by the alternate deposition of cesium and oxygen. For a current level of few  $\mu\text{A}$ , the quantum efficiency drops to  $\sim 80\%$  of its initial value after  $\sim 1000$  min.

### III. RESULTS AND DISCUSSION

#### A. Atomic hydrogen cleaning and photocathode performance

InP(100) samples, Zn doped to provide a carrier concentration of  $(2-3) \times 10^{18} \text{ cm}^{-3}$ , were used. Heavily *p*-doped InP samples were used since the Fermi level is close to the valence band and hence, electron emission by purely thermal excitation is minimized. The InP(100) was degreased in acetone and ethanol, with no chemical etching performed prior to loading the sample in UHV. The chamber was then baked for 48 h to achieve a pressure in the  $10^{-10}$  Torr range. The sample was kept at  $385^\circ\text{C}$  during the chamber bakeout, cooled down to room temperature, and then activated to NEA by the "yo-yo" technique.<sup>14</sup> Cesium was applied until maximum photocurrent response to 632.8 nm light was obtained, then oxygen was admitted which caused the photocurrent to drop. Cesium was then applied again until the photocurrent was maximized. This sequence was repeated, until there was no further improvement in the photocurrent. Figure 2 shows a typical "yo-yo" activation and QE, in response to 632.8 nm light for 1000 min. For a photocurrent level of few  $\mu\text{A}$ , the QE drops to  $\sim 80\%$  of its initial value after  $\sim 1000$  min. After the first activation, a QE of  $\sim 0.7\%$  was obtained for the freshly activated photocathode. Then, we exposed the sample to atomic hydrogen for 1 h cycles while the sample was kept at  $350-370^\circ\text{C}$ . After each cleaning cycle, the sample was cooled down to room temperature, activated again to NEA using the "yo-yo" technique, and the QE was measured for several hours. The QE increased after each cleaning cycle reaching a value of  $\sim 4\%$  after activation 8, as shown in Fig. 3. Then we continued with more hydrogen cleaning cycles, with the sample temperature raised to  $380-400^\circ\text{C}$ . After activation 10, the QE reached  $\sim 6.7\%$ . For other samples, we obtained a QE of  $\sim 8.5\%$  in response to 632.8 nm light. When we continued with more cleaning cycles, the QE remained between  $\sim 5.8\%$  and  $\sim 6.7\%$ . Before activations 16 and 18, we did not perform any atomic hydrogen irradiation; we revived the photocathode only by

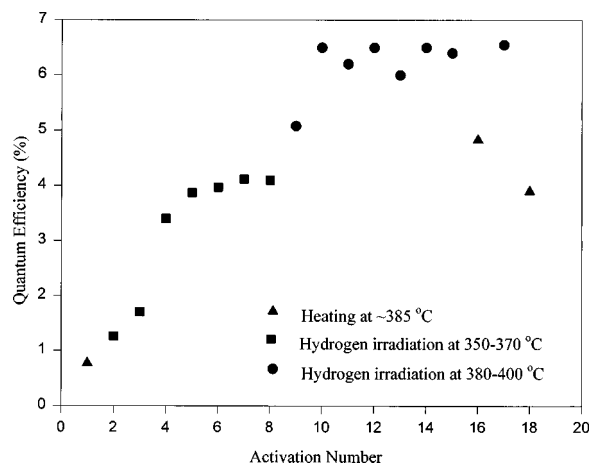


FIG. 3. The quantum efficiency of InP photocathode increases after atomic hydrogen cleaning. Samples kept at  $\sim 380-400^\circ\text{C}$  during atomic hydrogen cleaning give the highest quantum efficiency. Reviving by hydrogen irradiation produces photocathodes with higher quantum efficiency than those revived by heating only.

heating at  $385^\circ\text{C}$ . A QE of  $4\%-4.8\%$  was obtained. Results show that hydrogen cleaning is effective in the initial cleaning of InP prior to activation to NEA. When the InP samples are kept at  $380-400^\circ\text{C}$  during hydrogen cleaning, we obtain the best cleaning results. Atomic hydrogen is also effective in reviving the photocathode. The photocathode produces higher QE when revived with heating and atomic hydrogen irradiation than when revived with heating only.

#### B. Reflection high-energy electron diffraction studies

Next, we used RHEED to study the effect of heat and atomic hydrogen cleaning on the surface structure. Figure 4(a) shows the RHEED pattern of InP(100) after heat cleaning at  $385^\circ\text{C}$ . The electron energy was 8 kV, the angle of incidence of the electron beam was  $\sim 1.9^\circ$ , and the electron beam was incident along the  $\langle 0\bar{1}1 \rangle$  direction. In this case, no RHEED pattern can be seen, only a halo. This indicates that the surface is covered with a thick layer of amorphous oxides. Figure 4(b) shows a RHEED pattern after partial atomic hydrogen cleaning. Some features of the oxides can be seen, but no clear InP structure can be determined. Figures 4(c) and 4(d) show RHEED patterns after complete cleaning when the electron beam is along the  $\langle 0\bar{1}1 \rangle$  and  $\langle 011 \rangle$  directions, respectively. Clear  $(2 \times 4)$  reconstruction features can be observed indicating a phosphorus stabilized surface. The presence of well-defined diffraction spots falling on semi-circles indicates that the oxides on the surface are removed with little damage. Secondary features in the form of Kikuchi lines indicate the high quality of the bulk crystal. This surface produced the highest quantum efficiency ( $8.5\%$ ) in response to 632.8 nm light, when activated to NEA. The sample was then heated to the thermal cleaning temperature ( $\sim 530^\circ\text{C}$ ). This temperature is above the InP congruent temperature ( $\sim 400^\circ\text{C}$ ).<sup>3</sup> Figures 4(e) and 4(f) show RHEED patterns after heating the sample at  $530^\circ\text{C}$  for 30 min. The electron beam was incident along the  $\langle 0\bar{1}1 \rangle$  and  $\langle 011 \rangle$  directions, respectively. The patterns show diffraction spots, not streaks, indicating transmission features observed from

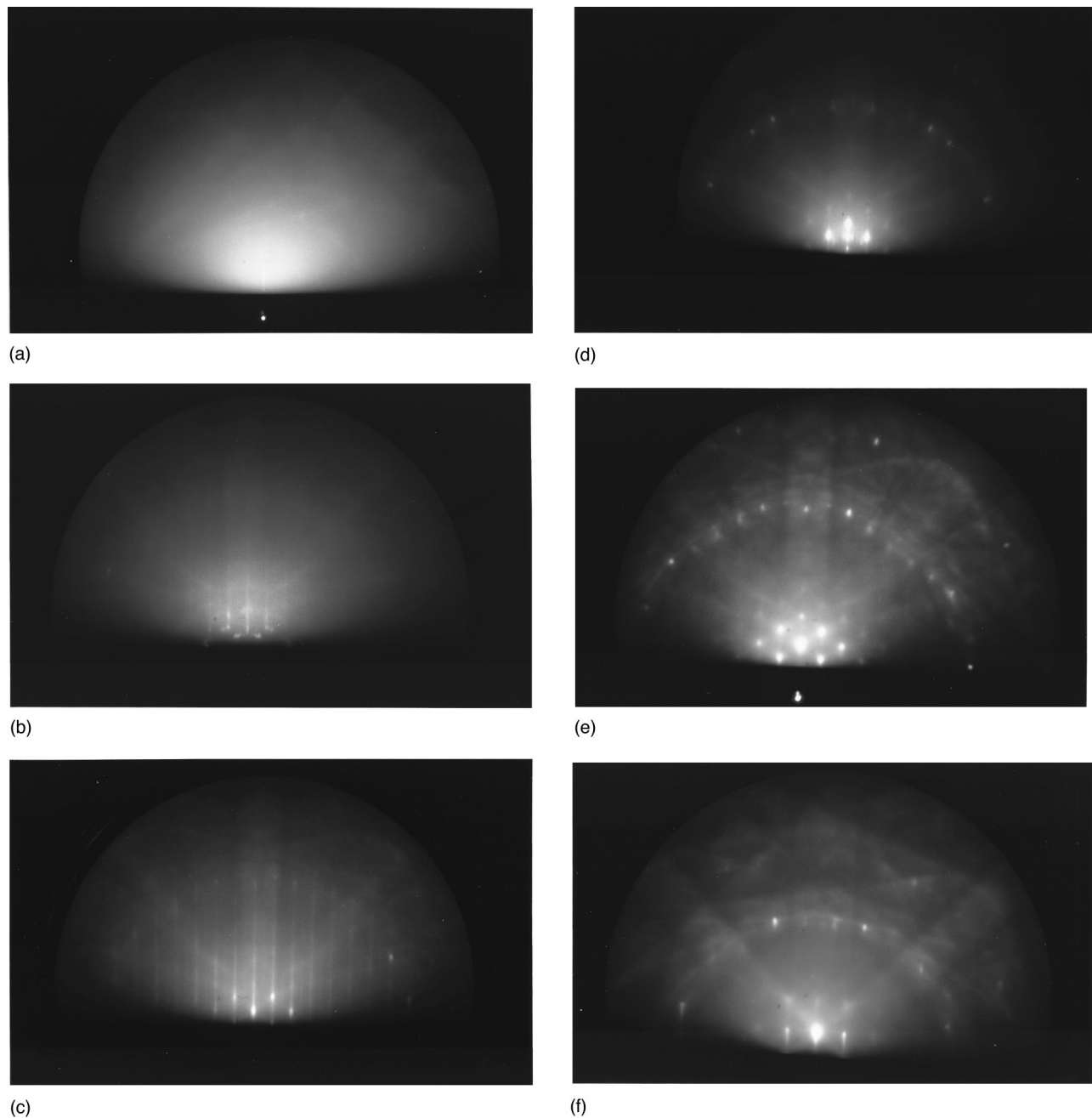


FIG. 4. Effect of hydrogen cleaning on RHEED patterns of InP(100). The electron beam is incident along  $\langle 0\bar{1}1 \rangle$  in (a), (b), (c), and (e), and along  $\langle 011 \rangle$  in (d), and (f). (a) Before hydrogen cleaning, no clear pattern is observed, only a halo, indicating a thick amorphous layer of oxides. (b) After partial atomic hydrogen cleaning, some oxide features are observed but no InP structure is seen. (c), (d) After atomic hydrogen cleaning and heating at  $\sim 400^\circ\text{C}$ . Clear reconstruction features are seen. (e), (f) After heating at  $530^\circ\text{C}$  showing transmission features indicating a rough surface.

rough surfaces. Above the congruent temperature, InP decomposes rapidly and phosphorus desorbs preferentially. This surface produced very low quantum efficiency ( $\sim 0.1\%$ ) in response to 632.8 nm light, when activated to NEA. The effect of atomic hydrogen on the InP surface was studied using Auger electron spectroscopy<sup>3</sup> and photoemission spectroscopy.<sup>18</sup> In the first stage, atomic hydrogen reacts with carbon compounds and the less stable indium oxide ( $\text{In}_2\text{O}_3$ ) and produces volatile compounds. Complete cleaning is limited by the removal of indium phosphate [ $\text{In}(\text{PO}_3)_3$ ] which requires long atomic hydrogen exposure.

We next show the use of RHEED to estimate the initial cesium layer thickness which maximizes the photocurrent before applying oxygen. The photocurrent was measured, and RHEED patterns were acquired every 30 s during cesium deposition. The initial RHEED patterns were clear and show a reconstructed surface. The angle of incidence of the electron beam was  $\sim 1.9^\circ$ , and the calculated electron penetration depth is  $\sim 0.6$  monolayer. When the cesium starts to cover the surface, the photocurrent increases, and the RHEED streaks start to disappear. As shown in Fig. 5, the intensity of the (01) RHEED streak decreases with cesium

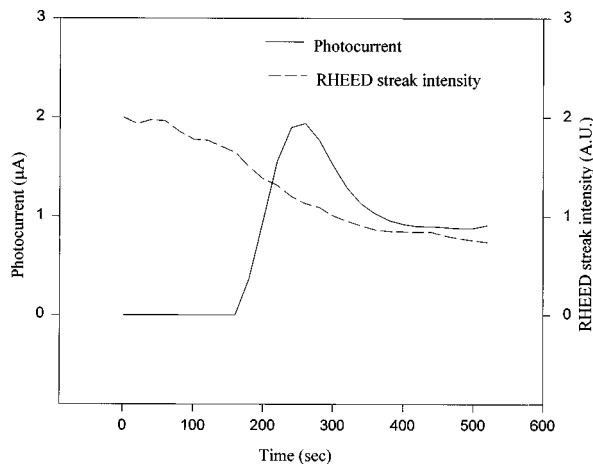
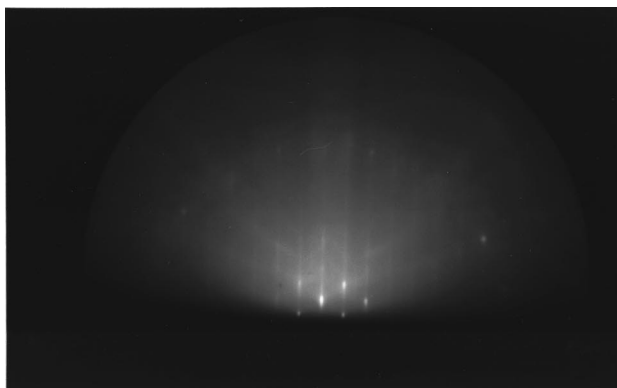
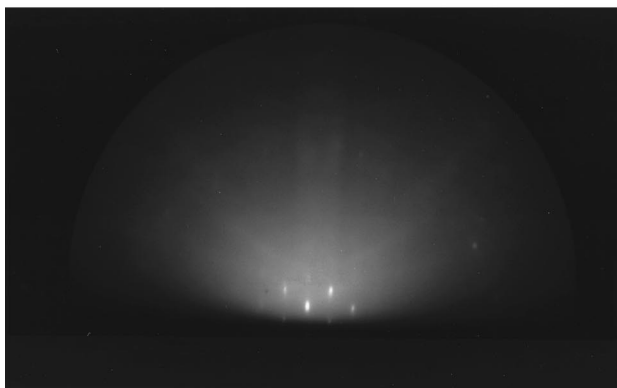


FIG. 5. The intensity of the (01) RHEED streak of InP(100) is used to determine cesium surface coverage. The photocurrent increases with cesium deposition, while the intensity of the RHEED streak decreases. The photocurrent reaches its maximum when the cesium coverage is  $\sim 0.5$  monolayer.

deposition. The photocurrent is maximum when the cesium thickness is  $\sim 0.5$  monolayer. Figures 6(a) and 6(b) show the RHEED patterns after 240 s and 480 s of cesium deposition, respectively. The intensity of the RHEED streaks decreases



(a)



(b)

FIG. 6. The intensity of the InP(100) (01) RHEED streak decreases with cesium deposition: (a) cesium deposition for 240 s, (b) for 480 s.

with cesium deposition. This demonstrates that RHEED can be effectively used to measure the cesium layer thickness on the photocathode and thus provides an effective way to control the cesium deposition rate.

#### IV. CONCLUSIONS

In conclusion, we prepared InP photocathodes using atomic hydrogen cleaning before activation to NEA. Atomic hydrogen reduces the cleaning temperature to 380–400 °C. This temperature is below the InP congruent temperature. Hence, this method produces a phosphorus stabilized, reconstructed surface. This surface, when activated to NEA, produced high QE photocathodes ( $\sim 8.5\%$ ). When the surface is heated to the cleaning temperature ( $\sim 530$  °C), phosphorus evaporates preferentially and the surface becomes rough as indicated by transmission RHEED patterns. This surface, when activated to NEA, produced very low QE photocathodes ( $\sim 0.1\%$ ). Atomic hydrogen cleaning was also shown to be effective in reviving the photocathode QE after its degradation with activation time.

- <sup>1</sup>K. J. Bachmann, *Annu. Rev. Mater. Sci.* **11**, 441 (1981).
- <sup>2</sup>V. L. Alperovich, Yu. B. Bolkhovityanov, A. G. Paulish, and A. S. Terekhov, *Nucl. Instrum. Methods Phys. Res. A* **340**, 429 (1994).
- <sup>3</sup>Y. Chun, T. Sugaya, Y. Okada, and M. Kawabe, *Jpn. J. Appl. Phys., Part 2* **32**, L287 (1993).
- <sup>4</sup>R. L. Bell, L. W. James, and R. L. Moon, *Appl. Phys. Lett.* **25**, 645 (1974).
- <sup>5</sup>R. L. Bell and J. J. Uebbing, *Appl. Phys. Lett.* **12**, 78 (1968).
- <sup>6</sup>T. Maloney, M. Burt, J. Escher, P. Gregory, S. Hyder, and G. Antypas, *J. Appl. Phys.* **51**, 2879 (1980).
- <sup>7</sup>R. La Rue, K. Costello, G. Davis, J. Edgecumbe, and V. Aebi, *IEEE Trans. Electron Devices* **44**, 672 (1997).
- <sup>8</sup>C. Sanford and N. MacDonald, *J. Vac. Sci. Technol. B* **7**, 1903 (1989).
- <sup>9</sup>E. Santos and N. MacDonald, *J. Vac. Sci. Technol. B* **11**, 2362 (1993).
- <sup>10</sup>E. Santos and N. MacDonald, *IEEE Trans. Electron Devices* **41**, 607 (1994).
- <sup>11</sup>D. T. Pierce, R. J. Celotta, G. C. Wang, W. N. Unertl, A. Galejs, C. E. Kuyatt, and S. R. Mielczarek, *Rev. Sci. Instrum.* **51**, 478 (1980).
- <sup>12</sup>F. Ciccacci, S. De Rossi, and D. Campbell, *Rev. Sci. Instrum.* **66**, 4161 (1995).
- <sup>13</sup>R. U. Martinelli and D. G. Fisher, *Proc. IEEE* **62**, 1339 (1974).
- <sup>14</sup>F. Ciccacci and G. Chiaia, *J. Vac. Sci. Technol. A* **9**, 2991 (1991).
- <sup>15</sup>F. Tang, M. Lubell, K. Rubin, A. Vasilakis, M. Emynan, and J. Slevin, *Rev. Sci. Instrum.* **57**, 3004 (1986).
- <sup>16</sup>J. Uebbing, *J. Appl. Phys.* **41**, 802 (1969).
- <sup>17</sup>E. Petit, F. Houzay, and J. Moison, *Surf. Sci.* **269/270**, 902 (1992).
- <sup>18</sup>T. Kikawa, I. Ochiai, and S. Takatani, *Surf. Sci.* **316**, 238 (1994).
- <sup>19</sup>S. V. Hattangady, R. A. Rudder, M. J. Mantini, G. G. Fountain, J. B. Posthill, and R. J. Markunas, *J. Appl. Phys.* **68**, 1233 (1990).
- <sup>20</sup>C. M. Rouleau and R. M. Park, *J. Appl. Phys.* **73**, 4610 (1993).
- <sup>21</sup>G. Bell, N. Kaijaks, R. Dixon, and C. McConville, *Surf. Sci.* **401**, 125 (1998).
- <sup>22</sup>Y. Okada and J. Harris, *J. Vac. Sci. Technol. B* **14**, 1725 (1996).
- <sup>23</sup>H. Shimomura, Y. Okada, and M. Kawabe, *Jpn. J. Appl. Phys., Part 2* **31**, L628 (1992).
- <sup>24</sup>N. Kondo, Y. Nanishi, and M. Fujimoto, *Jpn. J. Appl. Phys., Part 2* **31**, L913 (1992).
- <sup>25</sup>I. Suemune, Y. Kunitsugu, Y. Kan, and M. Yamanishi, *Appl. Phys. Lett.* **55**, 760 (1989).
- <sup>26</sup>K. Elamrawi and H. Elsayed-Ali (unpublished).
- <sup>27</sup>D. Barlett, C. W. Snyder, B. G. Orr, and R. Clarke, *Rev. Sci. Instrum.* **62**, 1263 (1991).
- <sup>28</sup>G. W. Wicks, E. R. Rueckwald, and M. W. Koch, *J. Vac. Sci. Technol. B* **14**, 2184 (1996).